Transient Stability Assessment of IEEE 9-Bus System Integrated Wind Farm

Ahmad Adel Alsakati[1], *Chockalingam Aravind* Vaithilingam[1,*], and *Jamal* Alnasseir[2]

[1]School of Computer Science and Engineering, Faculty of Innovation & Technology, Taylor's University, Malaysia
[2]Electric Power Engineering Department, Faculty of Mechanical & Electrical Engineering, Damascus University, Syria

Abstract. The use of wind energy is increased due to the high demand for sustainable energy. The penetration of wind energy in electrical networks might have several effects on load flow and power system stability. In this research, the transient stability of the IEEE 9-Bus system integrated with Doubly Fed Induction Generator (DFIG) is analyzed. Additionally, different penetration levels of a wind farm are considered. With a 5% penetration of wind energy, the maximum power angle of the synchronous generator is around 129 deg, which is quite similar to the existing system. In contrast, the power angle increases to 140 deg after adding more wind turbines with 15% wind farm penetration. Then, the system loses stability with a 25% penetration of wind energy. The results indicate that the high penetration of wind energy has a destabilizing impact on the studied network. Moreover, the location of the wind farm affects transient stability. This research intends to contribute towards assessing the stability of the power system integrated DFIG. Hence, this study will support the increase of using wind energy in power systems rather than conventional power plants and evaluate the stability to enable the reliability of alternative energy sources in the grid.

1 Introduction

Over the last two decades, the growing expansion in renewable energy has increased due to the environmental impacts [1], lack of fossil fuels, and growth in power demand [2]. The integration of renewable energy technology, such as photovoltaic and wind energy, into the network is a useful development to improve the power system performance [1]. Wind energy is one of the promising sources used in modern power systems [2,3]. The development of wind technology includes the increase in the rotor diameters and the height of towers [4]. In addition to the installation methods, there is another development in the type of generator to enhance the efficiency of the wind technology, such as squirrel cage induction generator and Doubly Fed Induction Generators (DFIG). In a squirrel cage induction generator, the capacitor is used to compensate for the reactive power [5]. In DFIG, the power is extracted when the wind speed is higher than the synchronous speed, and it is injected from the grid into the rotor when the wind speed is low. The DFIG is more common and popular among different wind turbine generators [6]. Wind energy relies on several factors, including the speed of the wind and weather. Thus, the variations in wind

* Corresponding author: aravindcv@ieee.org

speed have a large factor in changing the value of the power output [3]. The high penetration of wind energy may lead to power system issues, such as power system instability during the disturbances.

Power system stability is one of the most critical issues that should be addressed to increase the power system's reliability [7]. According to [8], the stability of a power system is the ability of the system to recover to an operating condition after disturbance. The stability of the power system can be categorized based on the physical nature of instability, size, and duration of disturbance [9]. The effects of power system stability issues are severe, such as blackout, load interruption, and limit transmission capacity [10].

In this research, the 9-Bus system is considered, and the high penetration level of wind energy with different locations is analyzed. Moreover, the impact of DFIG on transient stability is investigated. Power angles (angle differences) of synchronous generators are used to assess the transient state of the system. This research study highlights some of the barriers against the development of electrical power systems integrated wind energy. The paper is organized as follows; Section 2 presents the related works. The classification of power system stability is introduced in Section 3. Mathematical models and description of the studied network are presented in Section 4. Then, the results of the 9-Bus system integrated DFIG are discussed in Section 5. Lastly, Section 6 provides the conclusion and future work of this research study.

2 Related Work

The 9-Bus system is used in several works for power system analysis. Optimal power flow was applied to reduce the power losses of IEEE 9-Bus using ETAP [11]. The optimal method showed better results than the normal load flow method, and the fuel cost of the system was minimized. The Flexible AC Transmission Systems and adding a transmission line were used to improve the transient stability of the 9-Bus system during the fault [12]. The results indicated the effectiveness of these techniques to broaden the stability limit and increase the capacity of transmission lines. Authors in [13] have used critical clearing time to evaluate the stability of the power system. The effect of DFIG and thermal generator loading were investigated. Their results showed that the penetration of DFIG and the overloading of the thermal generator negatively affected transient stability. Another research has investigated power flow and contingency analysis [14]. Power and voltage of buses under normal conditions were used in their study to analyze the network. Line outage was used to analyze the contingency. Authors in [14] calculated the maximum loading factor and contingency status of 9-Bus system. They concluded that Line4-5 has the lowest loading parameter; by contrast, Line4-6 has the largest loading parameter.

Several models of wind turbines have been enhanced for increasing output power, developing control systems, and improving the efficiency of wind energy technology. There are two types of wind generator technologies that are mainly used in literature, Squirrel Cage Induction Generator (SCIG) and DFIG. Table 1 briefs the effect of two types of WTs on stability.

As seen in Table 1, the effects of wind turbines on stability vary, and these effects are associated with the type of generator and the control circuit using in the system. Moreover, DFIG has several advantages compared to other models, including that its control circuit can be used to improve stability.

Table 1. A brief overview of the wind turbines' effect on the oscillation.

SCIG	DFIG
It has a good impact on oscillation damping [15]. However, It may have a positive and negative influence on damping the oscillatory based on the location of wind turbine [16]	It has a good performance in damping the oscillations [16]
Induction generator without reactive power control may cause low-voltage issues [17]	Power control and DC-link voltage control are applied to DFIG [18]

3 Classification of Power System Stability

The stability of the power system can be categorized based on the physical nature of instability, the size, and the duration of disturbance [9]. Some types of stability events are described below.

3.1 Rotor angle stability

Rotor angle stability concerns the capacity of a power system to maintain a balance between electromagnetic torque and mechanical torque after having a disruption [8]. Rotor angle stability is divided into transient stability and small-disturbance stability. Transient stability is related to the capacity of the power system to keep synchronism when an extreme disturbance occurs, like a fault [19]. Small-disturbance stability is defined as the capability of power system to preserve synchronism under small disturbance [8,19].

3.2 Frequency stability

It describes the ability of the power system for keeping the frequency constant after disturbance [8].

3.3 Voltage stability

It describes the capacity of the power system to maintain steady-state voltages during normal conditions and after disturbance [8]. Voltage recovery is associated with many actions, such as Automatic Voltage Regulator (AVR), which controls the output voltage of the generators [20].

4 Methodology

In this section, the overall method for conducting the research is discussed. It consists of the mathematical models of the wind turbine, the penetration, and the locations of the wind farm. It also describes the 9-Bus system integrated with DFIG.

4.1 Wind turbine mathematical models

It is essential to measure the wind speeds in the selected area for at least one year before constructing wind turbines to harness the wind energy effectively [4]. Also, it is necessary

to study the mathematical models of wind turbines to calculate the potential extracted power from the wind [21]. The kinetic energy in the air is given by equation (1) [22].

$$K_E = \frac{1}{2} * m * V^2 \quad (1)$$

where *m* is air mass, which is flowing with wind speed *V*. The wind power defines as the amount of kinetic energy flows per second, it is given by equation (2) [22].

$$P = \frac{1}{2} * \frac{dm}{dt} * V^2 \quad (2)$$

Wind power is formulated by equation (3) [22,23].

$$P = \frac{1}{2} * \rho * A * V^3 \quad (3)$$

where ρ is air density, *A* is a swept area, and *V* is wind speed *m*/*s*.

The power coefficient Cp depends on the wind velocity in which the turbine operates. Moreover, the Cp value varies with the blade angle β and tip speed ratio λ. It is described by equation (4), and tip speed ratio is given in equation (5) [23,24].

$$C_p = f(\lambda, \beta) \quad (4)$$

$$\lambda = \frac{R * w}{V} \quad (5)$$

where R is the radius of the turbine, and w is the mechanical angular speed in rad/s. The tip speed ratio depends on wind speed and generator [25]. After considering the power coefficient, output power can be given by equation (6) [24,25].

$$P_{out} = \frac{1}{2} * \rho * A * C_p * V^3 \quad (6)$$

As observed from the above discussion, the output power from wind depends on some factors such as weather conditions, number, and length of blades [25].

4.2 Penetration and location of wind farm

Several factors should be discussed in the electrical network integrated wind energy. The location of a wind farm depends on economic and environmental factors [26]. In this research, different locations are investigated to determine suitable wind farm placement. In addition, three penetration levels of the wind farm are considered, that is, low-penetration, medium-penetration, and high-penetration, with levels 5%, 15%, and 25%, respectively. Wind Energy Penetration (WEP) is calculated by equation (7) [27].

$$WEP = \frac{WE}{WE+CPP} * 100\ \% \quad (7)$$

where CPP is the capacity of the conventional power plant in MW, and WE is the capacity of the wind farm in MW. In this paper, a 1.5 MW DFIG is chosen for each turbine; the voltage of wind generator is 575 V, the frequency is 60 HZ, and the inertia constant is 5.04 s. The parameters of DFIG are chosen from MATLAB Library. The method of connecting the wind turbine to the 9-Bus system is done using an example in MATLAB [28].

A wind farm consists of several wind turbines, which are connected to generate electricity. The output power of the wind farm is selected for different penetration levels. The output power of the wind farm is 18 MW, 60 MW, or 108 MW. In the studied network, the actual capacity of conventional power plants is around 321 MW. The penetrations of the wind farm for three different cases are calculated by using equation (7).

4.3 Generator models

The power system can be described by non-linear differential equations for a synchronous generator and the swing equation can be expressed as [29].

$$\frac{d\delta}{dt} = w - w_s \quad (8)$$

$$\frac{2H}{w_s}\frac{dw}{dt} = P_{mech} - P_e \quad (9)$$

where δ and w are power angle and speed of the synchronous generator. P_{mech} and P_e are mechanical and electrical power, respectively. H is the inertia time constant of the generator. The internal transient voltages, E'_d and E'_q, are given by equation (10) and equation (11) [29]

$$\frac{d\acute{E}_q}{dt} = \frac{1}{\acute{T}_{do}}\left(E_{fd} - \acute{E}_q - i_d(x_d - \acute{x}_d)\right) \quad (10)$$

$$\frac{d\acute{E}_d}{dt} = \frac{1}{\acute{T}_{qo}}\left(-\acute{E}_d + i_q(x_q - \acute{x}_q)\right) \quad (11)$$

where Efd is the excitation voltage, id and iq are stator currents on d-q axes. xd and xq are the d-q reactance, x'd and x'q are the transient reactance on d-q axes.

4.4 IEEE 9-bus modified system

A 9-bus system is a simple model used for stability analysis; it requires a small amount of data. Several articles and research works have discussed the normal operating conditions and transient stability study of the 9-Bus system [11–13,30,31]. In our research, the 9-bus modified system is considered and simulated through MATLAB R2019b. The system consists of three synchronous generators connected by a 230 kV transmission network. The parameters of transmission lines come from the literature [30,31]. The system is equipped with three generators rated 16.5 kV/247.5 MVA, 18 kV/192 MVA, and 13.8 kV/128 MVA [12,30,31]. The system contains three transformers to step up the voltage of each generator to 230 kV. It comprises three loads connected at bus 5, bus 6, and bus 8 [12,30,31]. The system has a fundamental frequency of 60 Hz. The synchronous generator is equipped with the governor, which is used to maintain the speed within specified limits. The turbine and governor are modelled with default parameters from MATLAB library. Also, the system is

integrated with the excitation system type DC1A [31]. The data of the 9-Bus system can be found in [12,30–32].

Faults were implemented in different locations to evaluate the power angle of synchronous generators. We found that the 3-phase fault simulated near Bus7 at Line5-7 has the largest power angles compared with faults occurred in other locations. The fault is cleared after 0.083 s and the faulty line is isolated by opening two circuit breakers. The power angle of Generator 2 and 3 with reference to Generator1 is considered to assess the transient stability [32,33]. If the power angle differences between generators decrease, the system is stable, however, if the power angle differences increase significantly, the generator will lose synchronism and the system is unstable [32,33]. Fig. 1 presents the IEEE 9-Bus modified system after modelled by MATLAB.

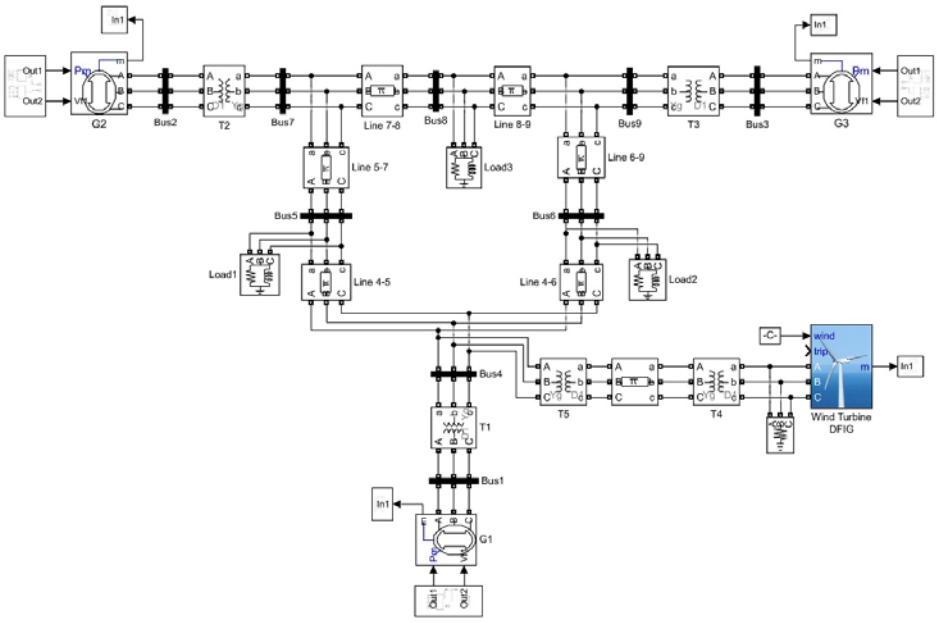

Fig. 1. Diagram of IEEE 9-Bus modified system integrated DFIG.

5 Result and Discussion

This section presents the voltage profile of the 9-Bus system during the three-phase fault on Line5-7 near Bus7. It also analyzes the transient stability of the studied network. Transient stability analysis considers power angle differences of synchronous generators. Several cases have been examined to investigate the effect of location and penetration of DFIG on transient stability.

5.1 Voltage profile

The 3-phase fault occurs in Line5-7 near Bus7. After 0.083 s, two circuit breakers are opened to isolate Line5-7. The voltage is stable before the fault. However, the voltage of Bus7 is zero during the fault, and the rest of the buses have been subjected to voltage droop. Fig. 2 shows the voltage of the buses.

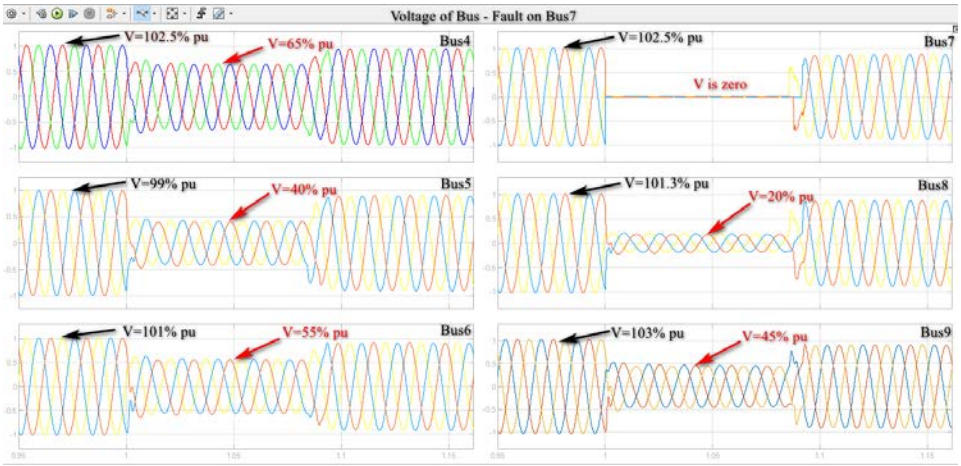

Fig. 2. Voltage profile before, during, and after the fault.

5.2 Transient stability analysis

5.2.1 Case 1 (existing system)

The 9-Bus system is considered without a wind turbine. The power angle differences of Generator2 and Generator3 are shown in Fig. 3. The power angles δ_{21} and δ_{31} increase to around 130° and 95°, respectively. Then, the following swings decrease to 94° and 68° for Generator2 and Generator3. In this case, the second swing was not higher than the first and the power angle reached maximum values and then reduced. Therefore, the system is stable with some oscillations.

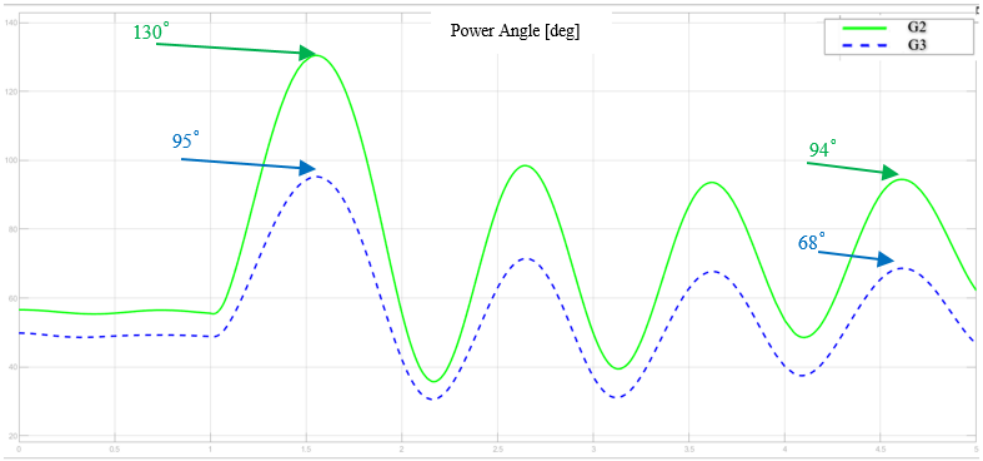

Fig. 3. Power angles δ_{21}, δ_{31} for the existing system.

5.2.2 Case 2 (5% penetration of wind energy added to Bus7)

A wind farm with a capacity of 18 MW is installed in Bus7. It includes 12 turbines, and each turbine generates 1.5 MW. Power angle differences of Generator2 and Generator3 are shown in Fig. 4. The power angles δ_{21} and δ_{31} increase to around 129° and 95°, respectively.

After the first swing, the power angles decrease to 90° and 65° for Generator2 and Generator3. As observed, there is a slight decrease in power angle after adding wind farm compared with the existing system.

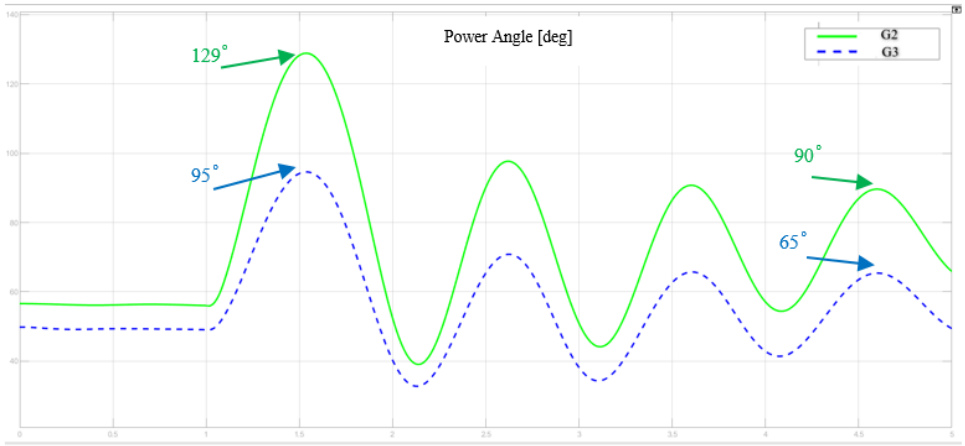

Fig. 4. Power angles δ_{21}, δ_{31} for 5% penetration of wind energy.

5.2.3 Case 3 (15% penetration of wind energy added to Bus7)

The wind farm with 60 MW output power is installed in Bus7. Power angle differences of generators are presented in Fig. 5. The power angles δ_{21} and δ_{31} increase to 140° and 103°, respectively. After the first swing, the power angles decrease to 101° and 72° for Generator2 and Generator3. It is noticeable that the power angle δ_{21} increases around ten degrees compared with the existing system.

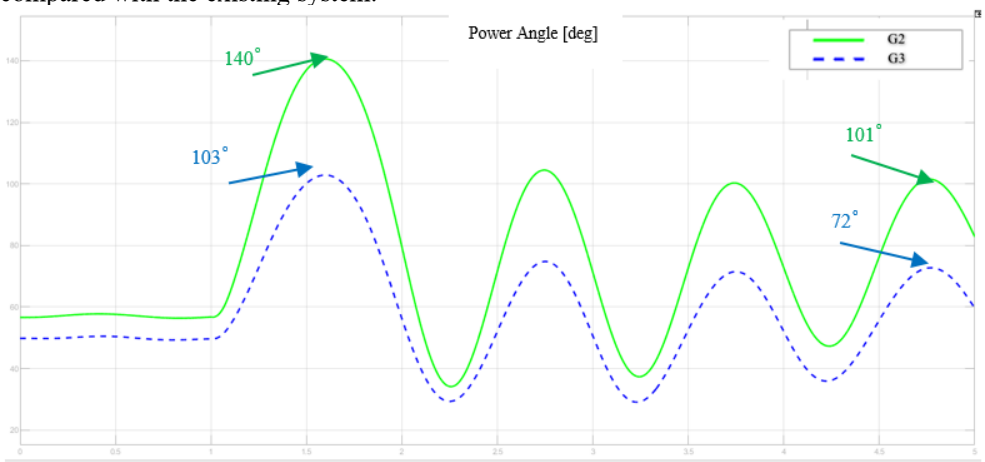

Fig. 5. Power angles δ_{21}, δ_{31} for 15% penetration of wind energy.

5.2.4 Case 4 (25% penetration of wind energy added to Bus7)

The wind farm with 108 MW output power is installed in Bus7. As observed in Fig. 6, the power angles of Generators increase significantly, and the system loses stability.

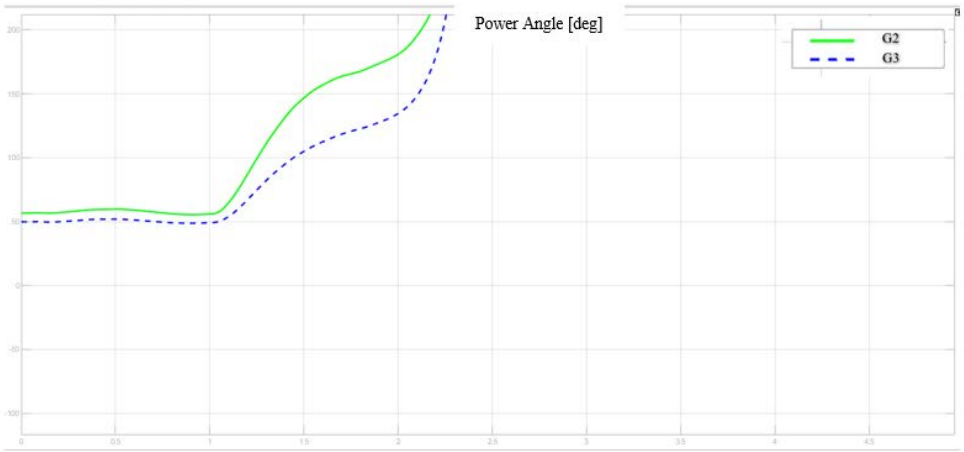

Fig. 6. Power angles δ_{21}, δ_{31} for 25% penetration of wind energy.

5.2.5 Case 5 (25% penetration of wind energy added to different locations)

In this case, different locations for a wind farm are investigated during the fault on Line5-7 near Bus7. The capacity of the wind farm is 108 MW, and the penetration of wind energy is around 25%. Fig. 7 shows the power angle δ_{21} when the wind farm is connected to Bus4, Bus5, Bus6, Bus7, Bus8, and Bus9 consecutively. As observed from the results, the power angle δ_{21} is the least when the wind farm is connected to Bus4 or Bus5. That is because the fault is far from the location of the wind farm, and the wind farm is connected near a swing generator. However, the power angle has the highest value when the wind farm is connected to Bus8. Therefore, Bus4 and Bus5 are suitable for implementing wind farm in terms of transient stability. The system is unstable when the wind farm is added to Bus7.

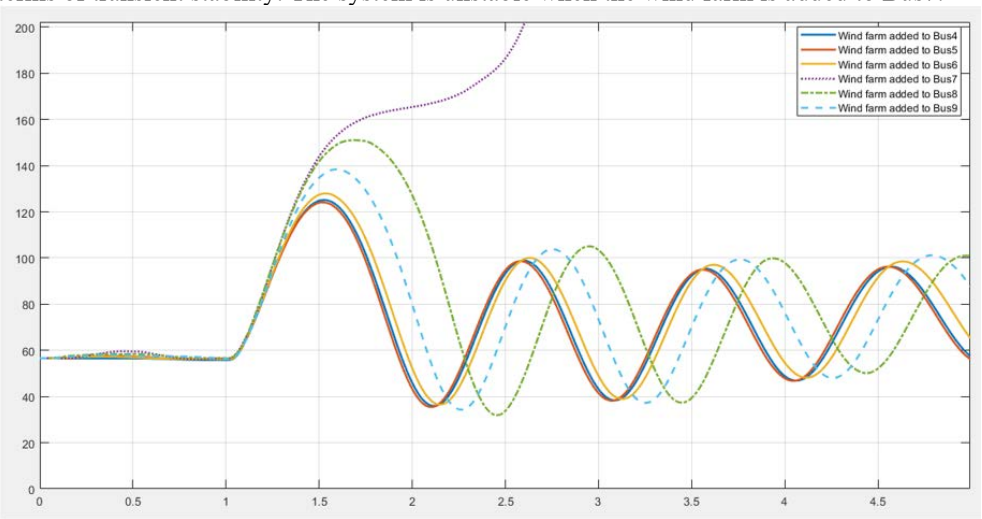

Fig. 7. Power angle δ_{21} for different locations of the wind farm.

6 Conclusions

In this paper, the effect of DFIG on the transient stability of the 9-Bus system is discussed. The time-domain simulation of the power angle is considered during the fault. The results have indicated that for the low penetration of wind energy, the power angle of synchronous generators is approximately the same as in the existing system. When the penetration level has increased to 25%, the system will most probably be unstable. The results also demonstrate that Bus4 and Bus5 are good locations to add wind farm in respect of transient stability. However, other factors should be considered to determine the location of wind farms, such as the probability distribution of wind speeds and economic feasibility studies, which were not within the scope of this research. In the future work for this research study, using an optimized intelligent Power System Stabilizer (PSS) can be considered. It is expected that the PSS controller will provide additional damping. Thus, it will allow to integrate wind energy with high penetration levels and ensure the reliability of renewable energy sources.

Acknowledgement: This work was supported by Taylor's University through its TAYLOR'S RESEARCH SCHOLARSHIP Programme (under Taylor's Research Grant Scheme, Project Reference No. TUFR/2017/001/01).

References

1. N. P. Gopinath, S. Prakash, O. K. S. Prakash, J. Suganthi. *2014* IEEE Nat Conf. Emer. Trends In New Renew. Energy Sour. Energy Manag. 186 (2014)
2. S. Sripadmanabhan Indira, C. Aravind Vaithilingam, K. S. P. Oruganti, F. Mohd, S. Rahman. Nanomater. **9**, 773 (2019)
3. C. V. Aravind, M. S. Khan, A. Saadha. J. Eng. Sci. Technol. **13**, 95 (2018)
4. O. Anaya-Lara, N. Jenkins, J. Ekanayake, P. Cartwright, M. Hughes, *Wind Energy Generation Modelling and Control* (A John Wiley & Sons, Ltd., UK, 2009)
5. P. He, F. Wen, G. Ledwich, Y. Xue. J. Mod. Pow. Sys. Clean Energy. **1**, 241 (2013)
6. F. Blaabjerg, Ke Ma. IEEE J. Emerg. Sel. Topics Power Electron. **1**, 139 (2013)
7. N. Cherif, A. Tayeb, B. Mokhtar. Int. J. Pow. Electron. Driv. Sys. **3**, 298 (2013)
8. P. Kundur, J. Paserba, V. Ajjarapu, G. Andersson, A. Bose, C. Canizares, N. Hatziargyriou, D. Hill, A. Stankovic, C. Taylor, T. V. Cutsem, V. Vittal. IEEE Trans. Power Syst. **19**, 1387 (2004)
9. B. S. Abdulraheem, C. K. Gan. Int. J. Appl. Eng. Res. **11**, 5688 (2016)
10. M. A. Hannan, N. N. Islam, A. Mohamed, M. S. H. Lipu, P. J. Ker, M. M. Rashid, H. Shareef. IEEE Access. **6**, 39574 (2018)
11. S. A. Kumar, M. S. S. Narayana, B. A. Naidu, G. V. S. Reddy. Int. J. Rec. Technol. Eng. **7**, 368 (2019)
12. R. Kaur, D. Kumar. MATEC Web Conf. 01026 (2016)
13. S. A. Kusumo, Tiyono, L. M. Putranto. ICITACEE, 61 (2018)
14. D. Asija, P. Choudekar, K. M. Soni, S. K. Sinha. RDCAPE, 338 (2015)
15. J. G. Slootweg, W. L. Kling. Elect. Power Sys. Res. **67**, 9 (2003)
16. T. R. Ayodele, A. A. Jimoh, J. L. Munda, J. T. Agee. ICREPQ'11, 244 (2011)
17. C. Chompoo-inwai, W.J. Lee, P. Fuangfoo, M. Williams, J.R. Liao. IEEE Trans. Ind. Appl. **41**, 163 (2005)
18. A. Tanvir, A. Merabet, R. Beguenane. Energies. **8**, 10389 (2015)
19. J. Bhukya, V. Mahajan. Int. J. Elect. Power Energy Sys. **108**, 314 (2019)
20. M. Ahmed, N. K. Roy. ICIEV. 797 (2016)

21. M. E. Abdallah, O. M. Arafa, A. Shaltot, G.A.A. Aziz. J. Elect. Sys. Inf. Technol. **5**, 121 (2018)
22. A. Ahmed, T. Jiang. ICCCEEE, 1 (2018)
23. A. B. Lajimi, S. A. Gholamian, M. Shahabi. Technol. Appl. Sci. Res. **1**, 121 (2011)
24. V. C. Ganti, B. Singh, S. K. Aggarwal, T.C. Kandpal. IEEE Trans. Sustain. Energy. **3**, 12 (2012)
25. C. V. Aravind, S. C. Tay, M. Norhisam, I. Aris, J. kumar. ICRESE. 248 (2013)
26. G. Kabashi, K. Kadriu, A. Gashi, S. Kabashi, G. Pula, V. Komoni. Int J Energy Pow. Eng. **5**, 161 (2011)
27. A. M. Khalil, R. Iravani. Int. J. Elect. Power Energy Sys. **104**, 827 (2019)
28. Wind Farm (DFIG Phasor Model) - MATLAB & Simulink, (Retrieved October 28, 2020)
29. S. Mishra, M. Tripathy, J. Nanda. Elect. Pow. Sys. Res. **77**, 1595 (2007)
30. M. Bey, M. Moudjahed. Bull. Elect. Eng. Inf. **5**, 8 (2016)
31. P. Jaikumar, IEEE 9 Bus Transient Stability Analysis, MATLAB Central File Exchange (Retrieved February 21, 2020) from www.mathworks.com/matlabcentral/fileexchange/66018-ieee-9-bus-transient-stability-analysis
32. P. M. Anderson, A. A. Fouad, *Power System Control and Stability*, Second Edition (A John Wiley & Sons, 2003)
33. P. Kundur, N. J. Balu, M. G. Lauby, *Power System Stability and Control* (McGraw-Hill, New York, 1994)